Chemistry of Metals and Alloys

Chem. Met. Alloys 4 (2011) 251-256
Ivan Franko National University of Lviv
www.chemetal-journal.org

The quasi-binary system $SmGa_2$–$SmAl_2$ at 600ºC

Taras SLIVINSKYY[1], Yaroslav TOKAYCHUK[1*], Karin CENZUAL[2], Roman GLADYSHEVSKII[1]

[1] *Department of Inorganic Chemistry, Ivan Franko National University of Lviv, Kyryla i Mefodiya St. 6, 79005 Lviv, Ukraine*
[2] *Département de Chimie Minérale et Analytique, Université de Genève, Quai Ernest Ansermet 30, CH-1211 Geneva, Switzerland*
** Corresponding author. Tel.: +380-32-2394506; e-mail: tokaychuk@mail.lviv.ua*

Received October 4, 2011; accepted December 28, 2011; available on-line August 17, 2012

Alloys of the quasi-binary system $SmGa_2$–$SmAl_2$ annealed at 600ºC were investigated by X-ray powder diffraction. Formation of a ternary compound, $SmGa_{1.00\text{-}0.75}Al_{1.00\text{-}1.25}$ (structure type AlB_2, Pearson symbol *hP*3, space group *P*6/*mmm*, *a* = 4.4463(2)-4.4784(2), *c* = 3.7646(2)-3.7230(2) Å) and substitutional solid solutions of the binary compounds, $SmGa_{2\text{-}1.32}Al_{0\text{-}0.68}$ (structure type AlB_2, *hP*3, *P*6/*mmm*, *a* = 4.235-4.2947(2), *c* = 4.183-4.1419(3) Å) and $SmGa_{0\text{-}0.21}Al_{2\text{-}1.79}$ (structure type $MgCu_2$, *cF*24, *Fd*-3*m*, *a* = 7.942-7.9283(2) Å), was established. Replacement of Ga atoms by Al atoms along the 33.3 at.% Sm isoconcentrate leads to an increase of the space-filling coefficient from 68.4 ($SmGa_2$) to 78.8 % ($SmAl_2$).

Samarium / Aluminum / Gallium / X-ray powder diffraction / Crystal structure / Solid solution

Introduction

Isothermal sections of the phase diagrams of ternary systems *R*–Ga–Al (*R* – rare-earth metal) have been constructed for the following rare-earth metals: Y, La, and Ce at 400°C in the region 0-33.3 at.% *R* [1,2], La at 400°C over the whole concentration range [3,4], Gd at 800°C in the region 20-100 at.% Gd [5,6], Ho at 500°C and 800°C in the region 25-33.3 at.% Ho [3]. For *R* = Ce [7], Nd [8,9], Eu [10], Gd [11], Er [8,9], Tm [12,13], and Yb [10,14] the quasi-binary sections RGa_2–RAl_2 have been investigated. In some systems, alloys of the equiatomic compositions *R*GaAl were synthesized and investigated by X-ray diffraction. This way *R*GaAl phases with the hexagonal AlB_2-type structure were found for *R* = Ce [15], Pr [16], Nd [8,9], Sm [17], Gd [17], Tb [17], Dy [18], Ho [19], and Er [8,9]. For the Yb-containing phase the structure type $CaIn_2$ was reported [10,14], whereas for the Eu- and Tm-containing phases the structure type KHg_2 was reported [10,13]. Crystallographic data for ternary phases reported in the quasi-binary systems RGa_2–RAl_2 are listed in Table 1.

The ternary systems *R*–Ga–Al are characterized by the formation of numerous ternary compounds with homogeneity ranges of different lengths along isoconcentrates of rare-earth metals, and solid solutions based on binary compounds. The ternary system Sm–Ga–Al has not yet been investigated. The only report on this system concerns the crystal structure of the phase SmGaAl [17], to which the structure type AlB_2 was assigned, but a complete structure refinement was not carried out. The crystal structures of the binary compounds are known and described in the literature: $SmGa_2$ (structure type AlB_2, Pearson symbol *hP*3, space group *P*6/*mmm*, *a* = 4.238, *c* = 4.187 Å) [21] and $SmAl_2$ ($MgCu_2$, *cF*24, *Fd*-3*m*, *a* = 7.940 Å) [22]. In the present article we report the results of a structural investigation of the quasi-binary system $SmGa_2$–$SmAl_2$ at 600°C, which is part of the phase diagram of the ternary system Sm–Ga–Al.

Experimental

13 ternary Sm-Al-Ga alloys containing 33.3 at.% Sm were synthesized by direct arc-melting of the constituent metals (Sm ≥ 99.83 wt.%, Al ≥ 99.985 wt.%, Ga ≥ 99.999 wt.%) under purified argon atmosphere. The samples were annealed at 600°C in evacuated quartz ampoules for 1 month and subsequently quenched in cold water. The weight loss during the preparation was less than 1 % of the total mass, which was 1 g for each alloy. Phase analysis was carried out using X-ray powder diffraction data collected on a diffractometer DRON-2.0M (Fe *K*α radiation) in the angular range $15 \le 2\theta \le 140^\circ$ with the step 0.05º. The profile and structural parameters were refined by the Rietveld method using the program package FullProf Suite [23]. For each phase the following parameters were refined: scale factor, unit-

Table 1 Ternary phases in the systems RGa_2–RAl_2.

Phase	Structure type	Pearson symbol	Space group	*a*, Å	*b*, Å	*c*, Å	Ref.
$YGa_{2-1.4}Al_{0-0.6}$	AlB_2	*hP*3	*P*6/*mmm*	4.20-4.25	–	4.10-4.07	[1]
$YGa_{1.3-1.1}Al_{0.7-0.9}$	AlB_2	*hP*3	*P*6/*mmm*	4.388-4.440	–	3.692-3.624	[2]
$LaGa_{2-0.3}Al_{0-1.7}$	AlB_2	*hP*3	*P*6/*mmm*	4.33-4.44	–	4.41-4.39	[1]
$CeGa_{2-0.9}Al_{0-1.1}$	AlB_2	*hP*3	*P*6/*mmm*	4.27-4.37	–	4.30-4.26	[1]
CeGaAl	AlB_2	*hP*3	*P*6/*mmm*	4.378	–	4.329	[15]
PrGaAl	AlB_2	*hP*3	*P*6/*mmm*	4.351	–	4.261	[16]
$NdGa_{2-0.86}Al_{0-1.14}$	AlB_2	*hP*3	*P*6/*mmm*	4.25-4.35	–	4.25-4.20	[8]
$NdGa_{2-0.85}Al_{0-1.15}$	AlB_2	*hP*3	*P*6/*mmm*	4.25-4.38	–	4.25-4.18	[9]
$NdGa_{0.86-0.54}Al_{1.14-1.46}$	AlB_2	*hP*3	*P*6/*mmm*	4.48-4.50	–	3.75-3.70	[8]
$NdGa_{0.84-0.50}Al_{1.16-1.50}$	AlB_2	*hP*3	*P*6/*mmm*	4.45-4.50	–	3.85-3.80	[9]
$NdGa_{0.35-0}Al_{1.65-2}$	$MgCu_2$	*cF*24	*Fd*-3*m*	8.01-8.00	–	–	[9]
$NdGa_{0.34-0}Al_{1.66-2}$	$MgCu_2$	*cF*24	*Fd*-3*m*	8.00-7.99	–	–	[8]
SmGaAl	AlB_2	*hP*3	*P*6/*mmm*	4.451	–	3.759	[17]
$EuGa_{2-0.8}Al_{0-1.2}$	KHg_2	*oI*12	*Imma*	4.644-4.682	7.640-7.716	7.625-7.717	[10]
$EuGa_{0.4-0}Al_{1.6-2}$	$MgCu_2$	*cF*24	*Fd*-3*m*	8.127-8.106	–	–	[10]
$GdGa_{2-1.4}Al_{0-0.6}$	AlB_2	*hP*3	*P*6/*mmm*	4.20-4.25	–	4.15-4.10	[11]
$GdGa_{1.2-0.8}Al_{0.8-1.2}$	AlB_2	*hP*3	*P*6/*mmm*	4.38-4.42	–	3.72-3.68	[11]
$GdGa_{0.2-0}Al_{1.8-2}$	$MgCu_2$	*cF*24	*Fd*-3*m*	7.90-7.90	–	–	[11]
TbGaAl	AlB_2	*hP*3	*P*6/*mmm*	4.434	–	3.637	[17]
$DyGa_{2-0.76}Al_{0-1.24}$	AlB_2	*hP*3	*P*6/*mmm*	4.197-4.449	–	4.029-3.571	[18]
HoGaAl	AlB_2	*hP*3	*P*6/*mmm*	4.444	–	3.555	[19]
$ErGa_{2-1.86}Al_{0-0.14}$	AlB_2	*hP*3	*P*6/*mmm*	4.22-4.22	–	4.00-4.00	[9]
$ErGa_{2-1.76}Al_{0-0.24}$	AlB_2	*hP*3	*P*6/*mmm*	4.40-4.40	–	4.03-4.03	[8]
$ErGa_{1.75-0.74}Al_{0.25-1.26}$	AlB_2	*hP*3	*P*6/*mmm*	4.32-4.42	–	3.65-3.50	[9]
$ErGa_{1.64-0.76}Al_{0.36-1.24}$	AlB_2	*hP*3	*P*6/*mmm*	4.40-4.45	–	3.60-3.50	[8]
$ErGa_{0.34-0}Al_{1.66-2}$	$MgCu_2$	*cF*24	*Fd*-3*m*	7.76-7.78	–	–	[8]
$ErGa_{0.34-0}Al_{1.66-2}$	$MgCu_2$	*cF*24	*Fd*-3*m*	7.72-7.77	–	–	[9]
$TmGa_{2-1.5}Al_{0-0.5}$	KHg_2	*oI*12	*Imma*	4.2021-4.2375	6.8874-6.9047	8.0752-8.0556	[12]
$TmGa_{2-1}Al_{0-1}$	KHg_2	*oI*12	*Imma*	4.210-4.270	6.886-6.912	8.070-8.040	[13]
$TmGa_{0.24}Al_{1.76}$	$MgCu_2$	*cF*24	*Fd*-3*m*	7.7585	–	–	[20]
$YbGa_{2-1}Al_{0-1}$	$CaIn_2$	*hP*6	$P6_3/mmc$	4.457-4.512	–	7.187-7.146	[10]
$YbGa_{2-1}Al_{0-1}$	$CaIn_2$	*hP*6	$P6_3/mmc$	4.450-4.500	–	7.200-7.160	[14]
$YbGa_{0.5-0}Al_{1.5-2}$	$MgCu_2$	*cF*24	*Fd*-3*m*	7.868-7.881	–	–	[10]
$YbGa_{0.5-0}Al_{1.5-2}$	$MgCu_2$	*cF*24	*Fd*-3*m*	7.868-7.875	–	–	[14]

cell parameters, profile parameters (pseudo-Voight profile function), occupancies and isotropic displacements parameters for all of the atoms. The background was defined by polynomial functions using a Fourier filtering technique.

Results and discussion

The X-ray phase analysis revealed a solid solution based on the binary compound $SmGa_2$, a ternary compound with a certain homogeneity range, and a solid solution based on the binary compound $SmAl_2$. The ternary compound crystallizes in the structure type AlB_2, and is consequently isostructural to $SmGa_2$. No indication for any of the numerous superstructures of AlB_2 was observed at the equiatomic composition, and the refinement of the site occupancies showed in all cases full occupancy of Wyckoff position 2*d* by a statistical mixture Ga/Al in agreement with the nominal composition. Between these phases there is a two-phase region. X-ray powder diffraction patterns collected from the thirteen ternary alloys are shown in Fig. 1. Patterns of single-phase samples from the solid solution based on the binary compound $SmGa_2$ are drawn in red, those from the homogeneity range of the ternary compound $SmGa_{1.00-0.75}Al_{1.00-1.25}$ in blue, and those from the solid solution based on the binary compound $SmAl_2$ in green. The binary compounds $SmGa_2$ and $SmAl_2$ dissolve 22.5 at.% Al and 7 at.% Ga, respectively, forming substitutional solid solutions with the formulas $SmGa_{2-1.32}Al_{0-0.68}$ and $SmGa_{0-0.21}Al_{2-1.79}$. The homogeneity range of the ternary phase is 8.4 at.% Ga or Al, leading to the composition $SmGa_{1.00-0.75}Al_{1.00-1.25}$. The concentration limits of the solid solutions based on the binary compounds and the homogeneity range of the ternary phase were determined from plots of the dependencies of the cell parameters on the composition (Fig. 2). Unit-cell parameters, average radii of the statistical

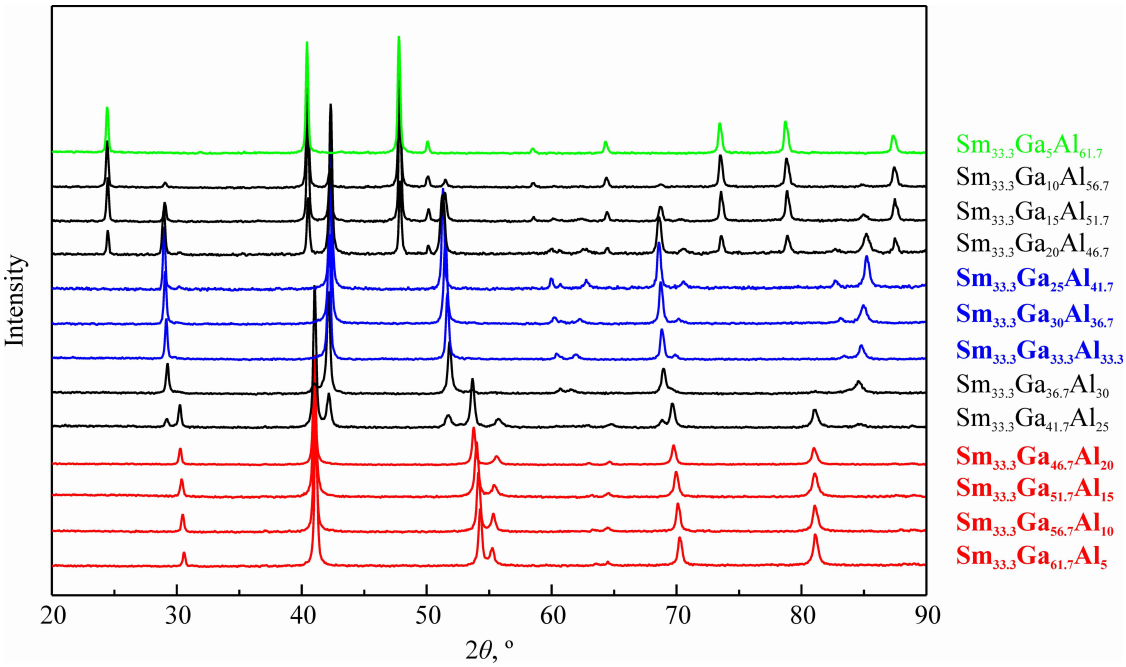

Fig. 1 X-ray powder diffraction patterns of the alloys of the quasi-binary system $SmGa_2$–$SmAl_2$.

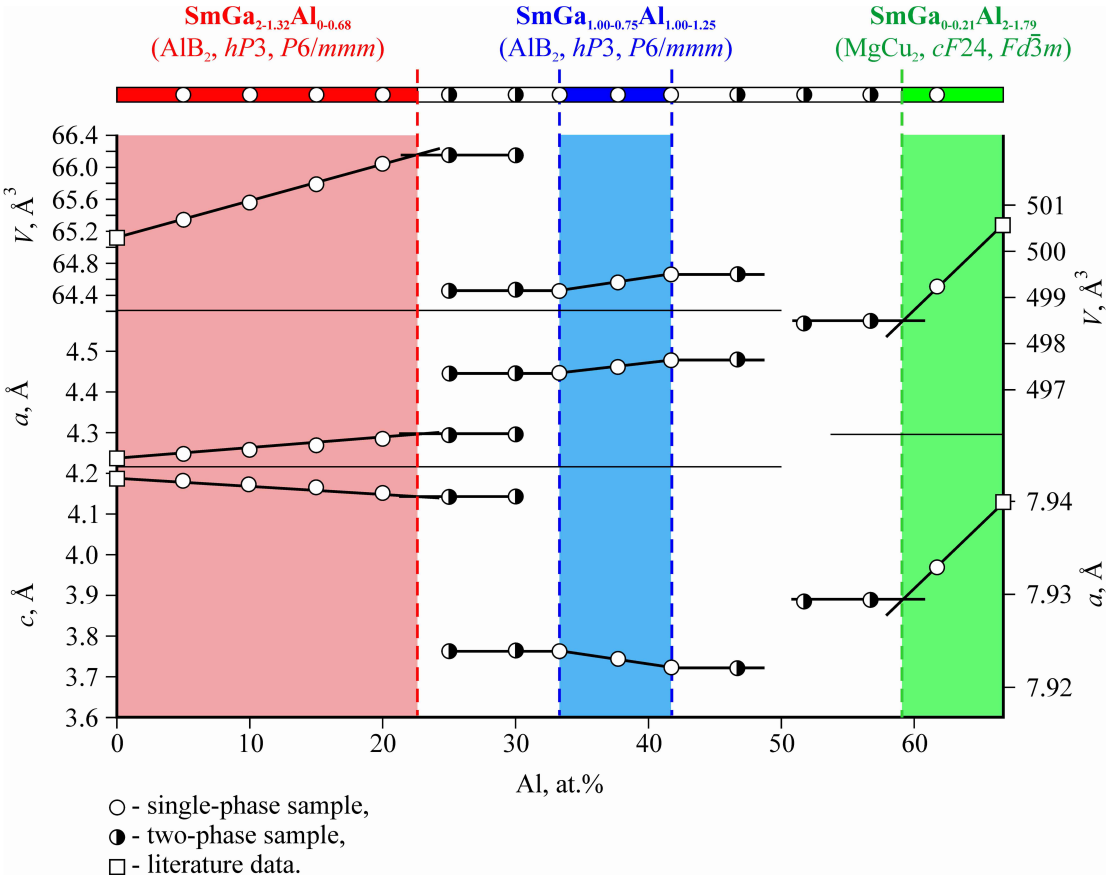

Fig. 2 Boundaries of the solid solutions based on the binary compounds $SmGa_2$ and $SmAl_2$, homogeneity range of the ternary compound $SmGa_{1.00-0.75}Al_{1.00-1.25}$, and the corresponding unit-cell parameters as a function of the Al content.

Table 2 Unit-cell parameters, average radii of the Ga/Al atoms and space-filling coefficient (*f*) for the phases that form in the $SmGa_2$–$SmAl_2$ system at 600ºC.

Alloy composition	Phase [a]	Structure type	Unit-cell parameters			*c*/*a*	$r_{(Ga/Al)}$, Å	*f*, % [b]
			a, Å	*c*, Å	*V*, Å^3			
–	$SmGa_2$ [21]	AlB_2	4.238	4.187	65.13	0.99	1.33	68.4
$Sm_{33.3}Ga_{61.7}Al_5$	$SmGa_2$	AlB_2	4.2499(17)	4.1815(2)	65.407(5)	0.98	1.337	68.6
$Sm_{33.3}Ga_{56.7}Al_{10}$	$SmGa_2$	AlB_2	4.2589(2)	4.1736(3)	65.560(6)	0.98	1.345	69.0
$Sm_{33.3}Ga_{51.7}Al_{15}$	$SmGa_2$	AlB_2	4.2703(2)	4.1664(3)	65.797(5)	0.98	1.353	69.3
$Sm_{33.3}Ga_{46.7}Al_{20}$	$SmGa_2$	AlB_2	4.2851(2)	4.1532(2)	66.045(5)	0.97	1.360	69.5
$Sm_{33.3}Ga_{41.7}Al_{25}$	$SmGa_2$ SmGaAl	AlB_2 AlB_2	4.2947(2) 4.4465(5)	4.1419(3) 3.7647(6)	66.160(8) 64.461(13)	0.96 0.85		
$Sm_{33.3}Ga_{36.7}Al_{30}$	$SmGa_2$ SmGaAl	AlB_2 AlB_2	4.2943(11) 4.4467(3)	4.1414(16) 3.7644(4)	66.16(3) 64.462(8)	0.96 0.85		
$Sm_{33.3}Ga_{33.3}Al_{33.3}$	SmGaAl	AlB_2	4.4463(1)	3.7646(2)	64.453(4)	0.85	1.380	72.7
$Sm_{33.3}Ga_{30}Al_{36.7}$	SmGaAl	AlB_2	4.4600(2)	3.7423(3)	64.500(7)	0.84	1.385	73.0
$Sm_{33.3}Ga_{25}Al_{41.7}$	SmGaAl	AlB_2	4.4784(2)	3.7230(2)	64.664(5)	0.83	1.393	73.4
$Sm_{33.3}Ga_{20}Al_{46.7}$	SmGaAl $SmAl_2$	AlB_2 $MgCu_2$	4.4789(2) 7.9287(9)	3.7233(2) -	64.685(6) 498.4(2)	0.83 1		
$Sm_{33.3}Ga_{15}Al_{51.7}$	SmGaAl $SmAl_2$	AlB_2 $MgCu_2$	4.4782(2) 7.9285(2)	3.7235(3) -	64.668(6) 498.39(2)	0.84 1		
$Sm_{33.3}Ga_{10}Al_{56.7}$	SmGaAl $SmAl_2$	AlB_2 $MgCu_2$	4.4785(4) 7.9289(2)	3.7238(6) -	64.682(14) 498.478(18)	0.84 1		
$Sm_{33.3}Ga_5Al_{61.7}$	$SmAl_2$	$MgCu_2$	7.9329(3)	-	499.23(3)	1	1.423	78.5
–	$SmAl_2$ [22]	$MgCu_2$	7.940	-	500.57	1	1.43	78.8

[a] $SmGa_2$ – solid solution based on $SmGa_2$ ($SmGa_{2-1.32}Al_{0-0.68}$), $SmAl_2$ – solid solution based on $SmAl_2$ ($SmGa_{0-0.21}Al_{2-1.79}$), SmGaAl – ternary compound $SmGa_{1.00-0.75}Al_{1.00-1.25}$;

[b] $f = \frac{\frac{4}{3}\pi(r_{Sm}^3 + 2r_{(Ga/Al)}^3)Z}{V} \cdot 100\%$, where r_{Sm} = 1.81, r_{Ga} = 1.33, r_{Al} = 1.43 Å, *Z* – formula units per cell, *V* – cell volume.

mixtures of Ga and Al atoms and space-filling coefficients for the phases that form in the $SmGa_2$–$SmAl_2$ system at 600ºC are listed in Table 2. With gradual replacement of Ga atoms by Al atoms in the isostructural phases $SmGa_{2-1.32}Al_{0-0.68}$ and $SmGa_{1.00-0.75}Al_{1.00-1.25}$ the cell parameter *a* increases, while the cell parameter *c* decreases. In both cases the unit-cell volume increases during progressive substitution of larger Al atoms for smaller Ga atoms. The *c*/*a* ratio for the solid solution $SmGa_{2-1.32}Al_{0-0.68}$ is close to 1 (≈ 0.98), while for the ternary compound $SmGa_{1.00-0.75}Al_{1.00-1.25}$ it is smaller than 1 (≈ 0.84).

Replacement of Ga atoms by Al atoms in the binary and ternary phases of the $SmGa_2$–$SmAl_2$ system leads to an increase of the space-filling coefficient from 68.4 to 78.8 % in the binary compounds $SmGa_2$ and $SmAl_2$, respectively. Within the homogeneity ranges the space-filling coefficient increases linearly, while between the phases it changes abruptly (Fig. 3).

As shown above, the replacement of smaller Ga atoms by larger Al atoms in the isostructural AlB_2-type phases leads to an increase of the cell parameter *a* and a decrease of the cell parameter *c*. This behavior can be explained by geometric features of the structure type AlB_2. The smaller atoms (Ga/Al) form graphite-like planar nets (Fig. 4a), located perpendicular to the *z*-axis (cell parameter *c*). With increasing average atomic radius of the statistical mixture Ga/Al, the cell parameters *a* and *b* increase due to the increase of the interatomic distances within the net. The Sm_6 trigonal prisms surrounding the Ga/Al atoms have their axes aligned along the *z*-axis (Fig. 4b). Their bases expand, but the height is reduced, leading to a decrease of the cell parameter *c*.

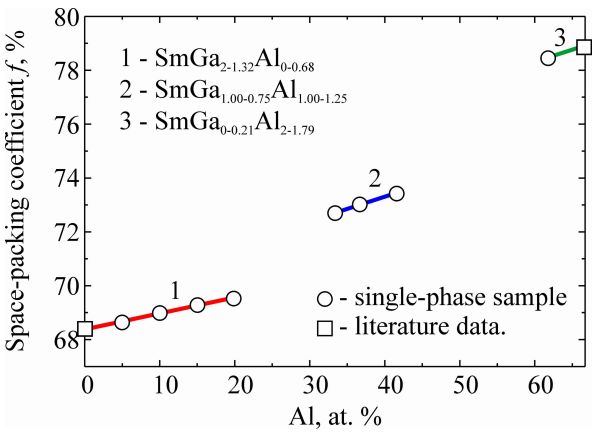

Fig. 3 Space-filling coefficient for the phases in the $SmGa_2$–$SmAl_2$ system as a function of the Al content.

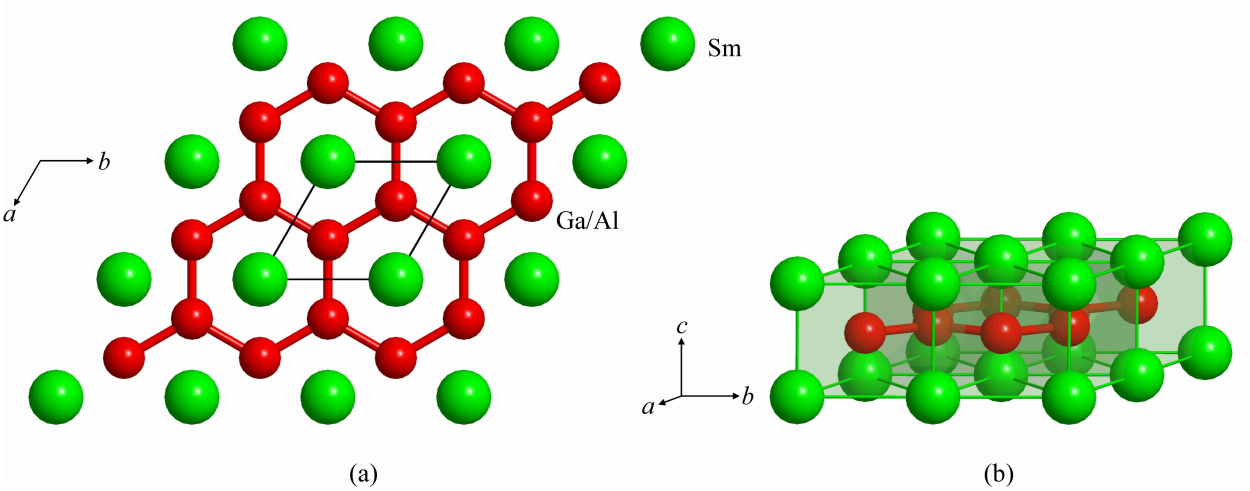

Fig. 4 Projection of a Ga/Al atom graphite-like planar net on the plane *ab* (a) and arrangement of trigonal prisms Sm_6 along *c* (b) in the structure of $SmGa_{2-1.32}Al_{0-0.68}$ (AlB_2 type).

The geometrically very simple structure type AlB_2 is conventionally subdivided into three branches according to the interaxial *c/a* ratio: *c/a* = 1.2-2.2, *c/a* = 0.9-1.2 and *c/a* = 0.5-0.9 [24]. The solid solution based on the binary compound $SmGa_2$ belongs to the second branch, where the atoms in Wyckoff position 1*a* have coordination number 12 (hexagonal prism) and the graphite-like net dominates the coordination of the smaller atoms (coordination number 3). The purely ternary phase including the composition SmGaAl belongs to the third branch. In this case the coordination of the rare-earth metal is increased from 12 to 14, since the two atoms capping the hexagonal faces of the prism are now at a similar distance. The rare-earth atoms become more important when considering the coordination of the smaller atoms (trigonal prism R_6), which also includes the two directly over- and underlying atoms of the same species (3+2+6). Even if "isostructural" to $SmGa_2$, the phase $SmGa_{1.00-0.75}Al_{1.00-1.25}$ thus represents an intermediate towards $SmAl_2$, where the coordination number of the Sm atoms is 16 (Friauf polyhedron) and that of the Al atoms 12 (icosahedron). The increase of the average coordination number corresponds to better space filling, whereas more local bonding should be present in $SmGa_2$. It can be seen from Table 1 that the same sequence of structure types is observed for the majority of the RGa_2–RAl_2 systems, whereas the systems with Eu and Yb constitute exceptions. The latter are more closely related to the corresponding systems formed by alkaline earth elements [10], showing once again the preference of these rare-earth elements for the two-valent state.

Conclusions

The quasi-binary system $SmGa_2$–$SmAl_2$ was investigated at 600°C by means of X-ray powder diffraction. The formation of substitutional solid solutions based on the binary compounds, $SmGa_{2-1.32}Al_{0-0.68}$ and $SmGa_{0-0.21}Al_{2-1.79}$, and an intermediate ternary compound was established. Substitution of Al atoms for Ga atoms in the binary and ternary phases of the $SmGa_2$–$SmAl_2$ system leads to an increase of the space-filling coefficient. Within the homogeneity ranges the space-filling coefficient increases linearly, while between the phases it changes abruptly.

Acknowledgements

This work was supported by Ministry of Education and Science, Youth and Sport of Ukraine under the grant No. 0109U002071.

References

[1] D.I. Dzyana, O.S. Zarechnyuk, *Visnyk Lviv. Univ. Ser. Khim.* 11 (1969) 8-10.
[2] M.V. Speka, V.Ya. Markiv, M.I. Zakharenko, N.M. Belyavina, *J. Alloys Compd.* 348 (2003) 138-145.
[3] V.V. Zavodyanyy, *PhD Thesis*, Taras Shevchenko Kyiv Univ., 1997.
[4] V.V. Zavodyanyy, V.Ya. Markiv, N.M. Belyavina, V.A. Makara, *Dopov. Akad. Nauk Ukr.* (8) (1997) 113-117.
[5] N. Golovata, O. Biloborodova, V. Markiv, N. Belyavina, *Coll. Abs. II Int. Conf. "Constructional and Functional Materials"*, Lviv (1997) 80-81.
[6] N.V. Golovata. *PhD Thesis*, Taras Shevchenko Kyiv Univ., 1999.
[7] A.Y. Takeuchi, S.F. da Cunha, *J. Alloys Compd.* 226 (1995) 126-130.
[9] O.E. Martin, K. Girgis, *J. Magn. Magn. Mater.* 37 (1983) 228-230.

[8] O.E. Martin, K. Girgis, A. Niggli, *J. Less-Comm. Met.* 75 (1980) 151-153.
[10] A. Iandelli, *J. Less-Comm. Met.* 135 (1987) 195-198.
[11] E. Talik, J. Heimann, A. Chelkowski, *J. Less-Comm. Met.* 124 (1986) L13-L16.
[12] C.H. Wang, K. Girgis, *J. Less-Comm. Met.* 158 (1990) 319-325.
[13] H. Lüscher, K. Girgis, P. Fischer, *J. Less-Comm. Met.* 83 (1982) L23-L25.
[14] L. Beck, K. Girgis, *J. Less-Comm. Met.* 109 (1985) 275-278.
[15] M.A. Fremy, D. Gignoux, D. Schmitt, A.Y. Takeuch, *J. Magn. Magn. Mater.* 82 (1989) 175-180.
[16] A. Garnier, D. Gignoux, J.L. de la Peña, D. Schmitt, *J. Magn. Magn. Mater.* 167 (1997) 52-56.
[17] A.E. Dwight, *Proc. 7th Rare Earth Res. Conf.*, Coronado, California, 1 (1968) 273-281.
[18] M. Doukoure, D. Gignoux, F. Saytat, *Solid State Commun.* 58 (1986) 713-718.
[19] D. Gignoux, D. Schmitt, A. Takeuchi, F.Y. Zhang, C. Rouchon, E. Roudaut, *J. Magn. Magn. Mater.* 98 (1991) 333-340.
[20] C.H. Wang, K. Girgis, O. Elsenhans, P. Fischer, *J. Less-Common Met.* 152 (1989) 171-175.
[21] S.E. Haszko, *Trans. Metall. Soc. AIME* 221 (1961) 201-204.
[22] J.H. Wernick, S. Geller, *Trans. Metall. Soc. AIME* 218 (1960) 866-868.
[23] J. Rodriguez-Carvajal, *Commission on Powder Diffraction (IUCr), Newsletter* 26 (2001) 12-19.
[24] G.O. Brunner, *Acta Crystallogr.* A33 (1977) 226-227.